PHYSICAL REVIEW E **83**, 060702(R) (2011)

Surface-induced reduction of twisting power in liquid-crystal films

LiDong Pan and C. C. Huang
School of Physics and Astronomy, University of Minnesota, Minneapolis, Minnesota 55455, USA
(Received 6 December 2010; published 20 June 2011)

Null transmission ellipsometry was employed to study the temperature evolution of the helical structure of the smectic-C^*_α phase. Free-standing films with thickness ranging from 31 to more than 400 layers were prepared and studied. The experimental results show a reduced twisting power in thin films. A simple model was constructed to explain the results. Surface effects were found to be the key reason for this phenomenon. Our findings are consistent with the theoretical studies of helically ordered magnetic films.

DOI: 10.1103/PhysRevE.83.060702 PACS number(s): 61.30.Hn, 77.84.Nh

Surface effects and finite size effects are unavoidable in experiments, since real systems are always finite and thus have boundaries. Finite size effects are known to shift the magnetic ordering temperature of thin films [1], while surface effects have been shown to produce their own critical behavior in the study of phase transitions [2]. Thus the studies of those effects are very important in the understanding of phase transitions in thin films as well as the behavior of nanoscale devices.

Liquid crystals provide excellent systems for studies of surface effects and finite size effects, especially smectic liquid crystals in which layered structures are found. In previous studies, those effects are found to shift the ordering temperature as well as change the phase transition behavior as the system sizes change [3–5]. In some other studies, completely new phases and structures are found in thin films which do not appear in bulk samples [6]. In many cases it is difficult to attribute one phenomenon to just the surface effects or the finite size effects. However, in a few examples, they lead to different aspects of the experimental results [7,8].

In the smectic-C^*_α (Sm C^*_α) phase, molecules are tilted away from the layer normal; the tilt direction of each layer is arranged in a helix along the layer normal, with pitch on the order of a few layers [9–11]. In a recent paper, we showed the similarities as well as differences between the Sm C^*_α and helically ordered magnetic films [8]. The finite size effect in both systems can be described within the same model and yield similar results.

Inspired by the recent studies of helically ordered magnetic films, in this paper we report our experimental results on the evolution of the Sm C^*_α structure in free-standing films with thickness ranging from 31 layers to more than 400. Our data show that as the film thickness decreases, the effective pitch of the helical structure increases. In contrast to previous results [11], a *buffer region* with reduced twisting power was discovered next to the surface region, and was found to be the result of surface effects. Although similar results were reported in computational studies of helically ordered magnetic films [12,13], so far, to our knowledge, no experiments have been able to demonstrate this effect. Thus our results will provide new insights and better understanding of surface effects, especially for layered systems.

The material used for this study is the antiferroelectric liquid crystal (AFLC) compound 10OTBBB1M7 (C10) [14]. Bulk C10 shows a smectic-*A* (Sm *A*) to Sm C^*_α transition at 124 °C (T_C). C10 was chosen for this study because we have detailed knowledge about the temperature evolution of the Sm C^*_α pitch in bulk samples from previous resonant x-ray diffraction (RXRD) experiments, providing a reference for the results in thin films [15].

The optical parameter Δ_+ (Δ_-) was acquired from our null transmission ellipsometer (NTE) as a function of temperature (T) with a weak in-plane external dc field **E** set to 90° (270°) from the incident laser direction. E was set to 6.25 V/cm, which is just strong enough to align the net polarization of the film without distorting the helical structure or inducing an electroclinic effect. The parameter Δ measures the phase difference between the *p* and *s* components of the incident light necessary to produce linearly polarized transmitted light. The light source is a He-Ne laser with wavelength $\lambda = 632.8$ nm. Free-standing films were prepared over a cover glass slide with an 8-mm-diameter hole in a temperature-controlled oven with stability better than ±15 mK. Argon is used as the exchange gas to minimize degradation of the sample. The detailed experimental setup was published elsewhere [16].

More than 40 films with different thicknesses were prepared in the ellipsometer in the Sm *A* phase. Following the procedure described in Ref. [7], optical parameters measured from those films at 129 °C were used in a 4×4 matrix method to obtain the values of the principal indices of refraction and layer spacing in the Sm *A* phase as $n_o = 1.490 \pm 0.005$, $n_e = 1.64 \pm 0.01$, and $d = 3.89 \pm 0.02$ nm. Those values are later used in the same fitting procedure to determine the thicknesses of the films studied.

Figure 1 shows the temperature evolution of the parameter Δ_+ obtained in cooling from films with thickness $N = 41$, 112, 184, and 322 layers. For this study cooling rates from 10 to 50 mK/min were used. In the Sm *A* window ($T - T_C > 0$), the parameter Δ_+ is almost temperature independent; while in the Sm C^*_α window ($T - T_C < 0$), Δ_+ shows oscillations, characteristic of the Sm C^*_α phase in free-standing films as explained in Refs. [10] and [11]. Also, it is evident from the figure that thicker films show more oscillations.

Before proceeding to data analysis, we need to understand the mechanism of the oscillations in Δ_+. For liquid crystals, surface-enhanced order usually produces a surface transition several degrees higher than the bulk transition [7,17]. For the case of the Sm *A*-Sm C^*_α transition, it means that several surface layers will be already tilted at T_C. However, in the Sm C^*_α phase, those biaxial surface layers do not join in the optically uniaxial helical structure of Sm C^*_α. As the pitch of

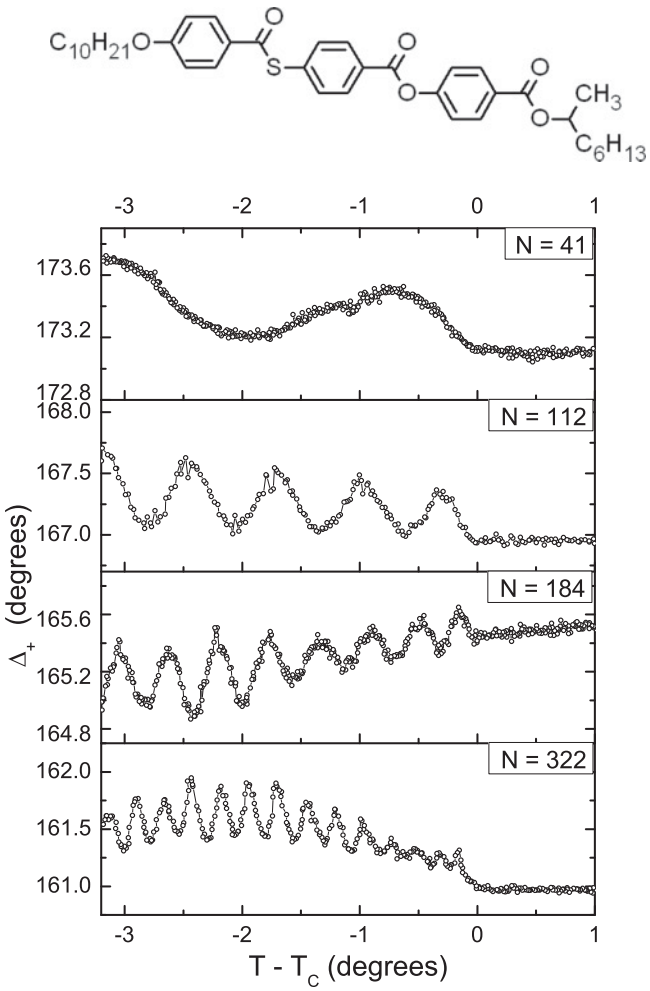

FIG. 1. $\Delta_+(T)$ from films with different N. The data are shown in the reduced temperature scale of the Sm A-Sm C^*_α transition. On the top is the chemical structure of C10.

the helix evolves with temperature, the two biaxial surfaces rotate at the same time, producing the observed oscillations. A complete oscillation is observed when the number of turns in the structure changes by 1 [10,11].

Since surface layers do not contribute to the formation of the helical structure in the Sm C^*_α phase, determination of the number of surface layers is a vital step. Figure 2(a) shows in log-log scale $\Delta_+ - \Delta_-$ measured at 129 °C (5 °C above T_C) from films with N ranging from 2 to more than 400 layers. It has been shown that, for planar structures, $\Delta_+ - \Delta_-$ is proportional to the total tilt angle of the film [4]. In Fig. 2(a) two distinct behaviors can be identified. For $N < 6$, an almost linear increase of $\Delta_+ - \Delta_-$ is observed as N increases; while for $N > 6$, $\Delta_+ - \Delta_-$ is almost flat. This feature clearly indicates that the surface order can be accounted for with a surface layer number $N_S = 3$. Thus for the Sm C^*_α structures in free-standing films of C10, there are three biaxial surface layers at each air-liquid crystal interface, with $N_{in} = N - 2N_S$ layers in the interior of the film. Biaxiality due to the incomplete helix in the interior is small compared to that from the surface layers.

Figure 2(b) shows the temperatures of the minima of the oscillations in Δ_+ from a 452-layer film over the Sm C^*_α window. The temperature of each minimum was obtained

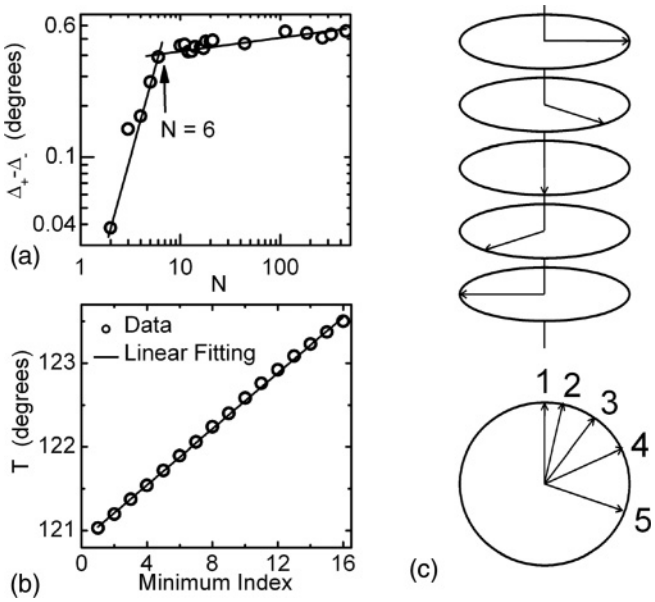

FIG. 2. (a) $\Delta_+ - \Delta_-$ measured at $T = 129\,^\circ$C from films with thickness N ranging from 2 to more than 400 layers plotted in log-log scale. (b) Temperatures of the oscillation minima in the Sm C^*_α window of the 452-layer film. (c) Cartoon (top) of the Sm C^*_α structure in the bulk with pitch of eight layers and top view (bottom) of the proposed structure of the *buffer region*; numbers are the layer index from the surface region.

by a parabolic fitting of the data near the minimum. The temperatures of the minimum locations can be described very well with a linear function. Thus the oscillation frequency over the temperature window concerned is constant. This agrees with the results from the RXRD data. So the oscillation behavior can be well described by the average frequency in temperature.

Figure 3 shows f_{norm}/N'_{in} as a function of N'_{in} for films with N ranging from 31 to 452 layers [18] ($N'_{in} = N_{in} - 1$, since between N layers there are $N - 1$ rotation angles). The frequency of the oscillation was obtained from the temperature and number of oscillations between the first and last discernible minima. f_{norm} was acquired by dividing the frequency of the oscillation by the corresponding value of the bulk sample ($f_{norm} = f/f_{bulk}$) [19]. The position of each minimum is again obtained from parabolic fitting.

Since the number of oscillations is given by the change of the number of turns in the helix, the frequency is proportional to the temperature derivative of $N'_{in}/P(T)$, with $P(T)$ being the pitch at temperature T. As a result, f_{norm}/N'_{in} is proportional to $1/P^2_{eff}$, where the effective pitch P_{eff} is the average number of layers in one complete turn of the helix. From Fig. 3, surprisingly, a decrease in f_{norm}/N'_{in} is observed as film thickness decreases. This observation is unexpected from previous understanding of the Sm C^*_α structure, which would suggest a constant average twisting power over the thickness studied. The decrease in f_{norm}/N'_{in} suggests an increase of effective pitch, i.e., a reduced twisting power of the helix in thin films. Since this effect is more pronounced in thin films, we expect surface effects and/or finite size effects to be the reason.

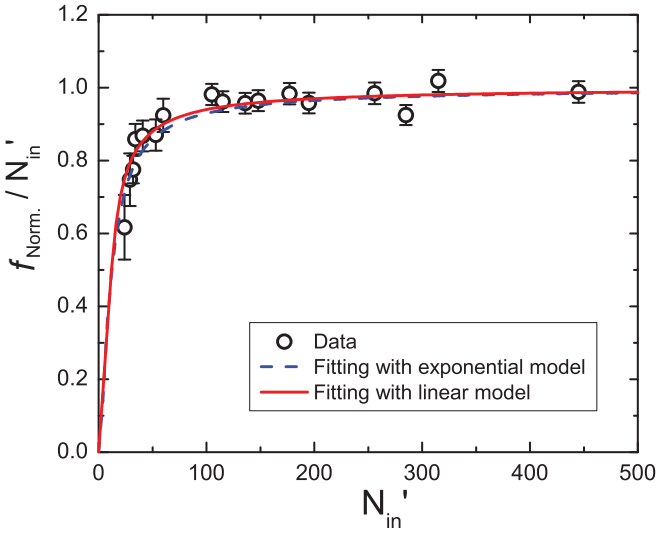

FIG. 3. (Color online) Data (symbols) and fitting with Eqs. (2) (solid line) and (3) (dashed line) of f_{norm}/N'_{in} plotted as a function of N'_{in}. Frequency is normalized by the bulk value.

To obtain further understanding and quantitative knowledge of the results, we first constructed a simple linear structural model. The model used is illustrated in Fig. 4 in open symbols. In our model, we assume that at each surface there are $N_S = 3$ surface layers that do not contribute to the formation of the helix; next to the surface layers, we have $N'_S = a$ layers of *buffer region* with rotation angle $\phi_a(i)$ smaller than the bulk value. The remaining part of the film (b layers, if $N > 2N_S + 2N'_S$) is assumed to have the bulk structure. In the buffer region, $\phi_a(i)$ is assumed to increases linearly from 0 to the bulk value ϕ_b as a function of the distance from the surface (i), so we have $\langle\phi_a\rangle = \phi_b/2$. A cartoon of the structure of the buffer region is shown in Fig. 2(c). Thus, the total rotation angle of the film is found to be

$$\phi_{total} = \begin{cases} (N'_{in} - a)\phi_b & \text{for } N_{in} \geqslant 2a, \\ (N'_{in}/2)^2\phi_b/a & \text{for } N_{in} < 2a. \end{cases} \quad (1)$$

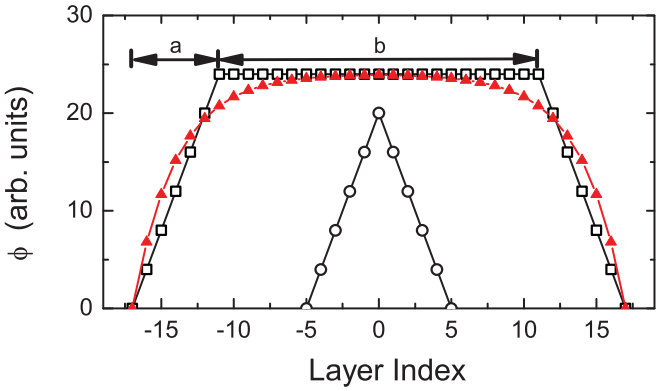

FIG. 4. (Color online) Structure of the model used in the text. Shown in open symbols is the rotation angle ϕ between two neighboring layers of the linear model for films with N_{in} greater (square) and smaller (circle) than $2a$, with the size of the buffer region $a = 6$ in the figure. Solid red triangle shows the ϕ profile of the exponential model with $\xi = 3$.

f_{norm}/N'_{in} is then given by [19]

$$\begin{cases} (N'_{in} - a)/N'_{in} & \text{for } N_{in} \geqslant 2a, \\ N'_{in}/4a & \text{for } N_{in} < 2a. \end{cases} \quad (2)$$

Thus, for films thicker than $2(N_S + N'_S)$, we have that f_{norm}/N'_{in} decreases slowly as N'_{in} decreases; while for thinner films, f_{norm}/N'_{in} is proportional to N'_{in}. The data can be described very well with the above equations as shown in Fig. 3. The best fit shown in Fig. 3 as a solid line gives $N'_S = 6$ layers for the data. Note that, in all our discussion, we assumed $N > 2N_S$.

We can also fit the data to an exponential structural model, with the rotation angle profile $\phi(i)$ given by $\phi_b[1 - \exp(-i/\xi)]$, where i is the distance from the surface region, and ξ is a characteristic length of the model. This model is illustrated in Fig. 4 with solid symbols. Here we have

$$f_{norm}/N'_{in} = 1 - \frac{2}{N'_{in}}\left(\frac{1 - e^{N'_{in}/2\xi}}{1 - e^{1/\xi}}\right). \quad (3)$$

This model produces almost identical behavior as the linear model. The best fit shown in Fig. 3 as the dashed line gives $\xi =$ 3 layers. However, as shown in Fig. 4, the linear model gives a more straightforward estimate of the size of the buffer region.

Our data were also analyzed with a different method. We studied the dependence of the oscillation frequency on N. The relation between those two quantities can be described with a linear function, with the intercept on the thickness axis $N_0 = 13$ layers. This result is consistent with the previous result from fitting the data in Fig. 3 with Eq. (2). Since in our model we have $\langle\phi_a\rangle = \phi_b/2$, if we treat the whole film as consisting of only the surface region which does not contribute to the helix and interior region that is bulklike, the two-buffer region ($2N'_S$ with $\langle\phi_a\rangle$) will contribute the same ϕ_{total} as N'_S layers with ϕ_b; thus we will have an effective total surface thickness $2N_{S\,eff} = 2N_S + N'_S = N_0$, namely, we should have $2N_{S\,eff} = 6 + 6$ layers $\approx N_0$. The excellent match of the results from two different methods suggests that the structural model we used is a very good representation of the system.

In a recent paper [8], we demonstrated that the finite size effects on the stability of both the Sm C^*_α phase in AFLCs and helically ordered magnetic films can be understood with the same phenomenological model. The formation of the helical structure in both systems can be viewed as the result of competition between the ferromagnetic (FM) nearest neighbor (NN) interlayer interaction and the antiferromagnetic (AFM) next nearest neighbor (NNN) interlayer interaction (for the case of AFLCs, the corresponding interactions are the ferroelectric NN and antiferroelectric NNN interlayer interactions). Due to the fact that near the surfaces there are fewer NNN interlayer bonds than NN interlayer bonds, we have a reduced weight of the AFM NNN interlayer interaction as compared to the FM NN interlayer interaction. As a result, near the surfaces the rotation angle ϕ between the magnetic moments in neighboring layers (for the Sm C^*_α case, ϕ is the angle between the tilt direction of molecules in neighboring layers) is smaller compared to the interior value, i.e., near the surface region there is a tendency toward FM alignment, and the closer to the surface, the smaller ϕ will be.

The above discussion provides briefly the reasoning of our model. While this structure was suggested in several computational studies of helically ordered magnetic thin films [12,13], at this moment there is no direct experimental evidence available. With the demonstrated similarities between the Sm C^*_α phase and the helically ordered magnetic films, our study constitutes an experimental confirmation of the main computational results reported for the magnetic system. However, the easy preparation of smectic films with desired thickness without the need for substrates makes this system experimentally more accessible. Our results also demonstrate that the properties and many different structures of AFLCs make them an excellent system for the study of surface effects and finite size effects in layered systems.

It is interesting to see from our results that the buffer region is larger than the surface region; we have $N'_S = 2N_S$. This suggests a strong surface-induced aligning field in liquid crystal free-standing films. The aligning field in this region is probably produced by the planar biaxial surface layers [20]. The mechanism of this surface field and its long effective range is beyond our work and calls for future theoretical studies.

In summary, we studied the thickness-dependent evolution of the helical structure of the Sm C^*_α phase, and discovered a large buffer region with reduced rotation angle ϕ. This is probably due to the aligning field produced by the biaxial surface layers. From our results, we now have a much better picture of the structure of the Sm C^*_α phase in free-standing films. Next to the biaxial surface layers at the air-liquid crystal interface that do not contribute to the helix, there are several layers of buffer region, in which the rotation angle ϕ is smaller than the bulk value. The rest of the film shows the bulk structure. Our results also provide experimental evidence supporting the computational work reported for helically ordered magnetic films.

This research was supported in part by the National Science Foundation, Solid State Chemistry Program, under Grant No. DMR-0605760. L.D.P. acknowledges financial support from University of Minnesota Graduate School, under the DDF program. The authors would like to thank Dr. H. T. Nguyen for supplying the high-quality C10 compound.

[1] P. J. Jensen and K. H. Bennemann, Surf. Sci. Rep. **61**, 129 (2006).
[2] K. Binder, in *Phase Transitions and Critical Phenomena*, edited by C. Domb and J. L. Lebowitz (Academic, New York, 1983), Vol. 8, p. 1.
[3] P. Sheng, Phys. Rev. A **26**, 1610 (1982).
[4] Ch. Bahr and D. Fliegner, Phys. Rev. A **46**, 7657 (1992).
[5] T. Bellini *et al*., Science **294**, 1074 (2001).
[6] E. B. Sirota *et al*., Phys. Rev. A **36**, 2890 (1987).
[7] L. D. Pan *et al*., Phys. Rev. E **79**, 031704 (2009).
[8] L. D. Pan *et al*., Phys. Rev. Lett. **103**, 187802 (2009).
[9] P. Mach *et al*., Phys. Rev. Lett. **81**, 1015 (1998).
[10] D. Schlauf, C. Bahr, and H. T. Nguyen, Phys. Rev. E **60**, 6816 (1999).
[11] P. M. Johnson *et al*., Phys. Rev. Lett. **83**, 4073 (1999).
[12] E. Weschke *et al*., Phys. Rev. Lett. **93**, 157204 (2004).
[13] F. Cinti, A. Cuccoli, and A. Rettori, Phys. Rev. B **79**, 134420 (2009).
[14] The phase sequence reported for bulk C10 is isotropic (153 °C)–Sm *A* (124 °C)–Sm C^*_α (120 °C)–Sm C^* (119 °C)–Sm C^*_{d4} (114 °C)–Sm C^*_{d3} (112 °C)–Sm C^*_A (110 °C)–crystal. However, no Sm C^* phase was observed using either RXRD or NTE.
[15] In our RXRD experiments, we found that bulk C10 shows a pitch evolution almost linear in temperature in the Sm C^*_α window, with pitch equal to 8.15 layers at 122.77 °C and 5.81 layers at 119.2 °C.
[16] D. A. Olson *et al*., Liq. Cryst. **29**, 1512 (2002). Also, with the advances in our instrumentation over the years, now much improved results can be achieved from the thin films studied.
[17] L. D. Pan *et al*., Phys. Rev. Lett. **105**, 117802 (2010).
[18] The 31-layer film is the thinnest film studied, for it showed just more than one-half oscillation.
[19] The frequency is given by $\Delta\phi_{total}/(2\pi\,\Delta T)$; from Eq. (1), it is easy to arrive at Eq. (2), with $\Delta\phi_b/(2\pi\,\Delta T)$ being the bulk value used as reference for the normalization (f_{bulk}). ΔT is the temperature range of the Sm C^*_α phase.
[20] The anisotropy of the elasticity created with the biaxial surface layers could be one of the candidate mechanisms for the aligning field; see M. B. Hamaneh and P. L. Taylor, Phys. Rev. Lett. **93**, 167801 (2004).